Journal of Fluids and Structures (1998) **12,** 315–333

ENERGY FLOW ANALYSIS OF BEAMS AND PLATES FOR RANDOM DISTRIBUTED LOADING

F. Han, L. G. Mongeau and R. J. Bernhard

Ray W. Herrick Laboratories, School of Mechanical Engineering, Purdue University West Lafayette, IN 47907-1077, U.S.A.

(Received 15 May 1997 and in revised form 18 November 1997)

The time- and frequency-averaged energy response of beams and plates excited by a random distributed loading was investigated. Two methods for calculating the input power density from the cross-spectral density of the distributed excitation were developed, used, and compared. The energy response was calculated using energy flow analysis and modal analysis. Assuming the input impedance was that of comparable structures of infinite extent, energy flow analysis was found to yield energy density predictions in good agreement with the spatially averaged energy density response obtained using modal analysis and exact transfer functions for the power density input estimation. The benefits of this approach are discussed for the case of a simply supported plate excited by a turbulent boundary layer wetting only half of the span of the plate.

1. INTRODUCTION

The dynamic response of extended structures and acoustic media subject to high-frequency broadband excitation is of interest in situations where vibration is induced by unsteady, turbulent flows. Examples of this problem include structural fatigue and excessive noise emissions for a wide range of applications, such as road vehicles, aircraft, propulsion systems, fluid-moving machinery, and piping systems. The complexity of high-frequency dynamic interactions between turbulent fluid flow, complex vibrating structural networks, and sound radiation within reflecting boundaries usually precludes the use of detailed numerical or analytical models. Good approximate models are needed to guide design and assess structural integrity and sound quality. One possible approach is to use energy variables to describe these dynamic interactions in a manner analogous to heat exchange phenomena in complex, built-up thermal systems.

This study is focused on the vibration response of flow-excited structures that are driven over a spatially distributed region much greater in size than a typical wavelength of bending waves in structures. Average estimates of the response are useful at high frequencies when wavelengths are short, and thus, the spatially averaged response is generally a good indicator of the behaviour of a system. Energy methods to predict the space- and frequency-averaged behaviour of such structures include energy flow analysis (EFA) and statistical energy analysis (SEA). For SEA approximations, lumped parameters are used to represent a continuous system. The solution estimates a single energy value for each subsystem. The governing differential equations of EFA are derived using a differential volume approach. The equations allow the spatial variation of the space- and frequency-averaged energy density and energy flow to be predicted. In addition, EFA can be implemented using

0889-9746/98/030315 + 19 $25.00/fl970136

a finite-element method. The resulting energy finite-element method (EFEM) allows high-frequency predictions to be made using finite-element models developed for low-frequency structural response predictions. This can result in considerable time and cost savings. The application of the EFA method to simple harmonic, locally excited structures has been verified for rods and beams (Wohlever & Bernhard 1992), membranes (Bouthier & Bernhard 1995*a*) and plates (Bouthier & Bernhard 1995*b*). The approach was extended to random, locally excited beams and plates by Han *et al.* (1997). The results were shown in most cases to be a satisfactory approximation of the exact solution.

The purpose of this study is to investigate the energy response of structures to flow excitations, whereby turbulence and other flow fluctuations impose a randomly distributed pressure field over a significant region of the structure. The surface pressure fluctuations may be spatially coherent, incoherent or partially coherent depending on the nature of the flow near the walls. The energy flow analysis method requires input power density data to characterize the excitation. For this, the cross-spectral density of the pressure field between any two different points of the structure is needed. Two methods were developed to calculate the power density input from cross-spectral density information: (i) a "transfer function" method, where analytical expressions for the response of the actual structure, including the effects of boundaries, were used; and (ii) an "impedance" method, where the input impedance of the structure was estimated to be that of a comparable structure of infinite extent.

The predictions of the energy response of beams and plates using EFA and the newly developed input power density methods were compared to energy solutions obtained in terms of transverse displacement using a formal modal summation approach. The methods for calculating the input power densities and energy responses were also used to predict the response of a plate excited by a turbulent boundary layer wetting only half of the span of the plate. The results suggest that EFA and EFEM methods for distributed random loading yield energy density predictions that are accurate with intrinsically better spatial resolution than available from SEA models.

2. POWER DENSITY INPUT TO BEAMS AND PLATES

Two methods for calculating the power input for locally excited beams and plates, the transfer function method and the impedance method, have been developed in a previous paper (Han *et al.* 1997). These are extended here to the case of distributed loading.

2.1. The Transfer Function Method

A schematic of a simply supported beam excited by a random distributed pressure loading $p(x, t)$ is shown in Figure 1. The input power density at position x can be expressed in terms

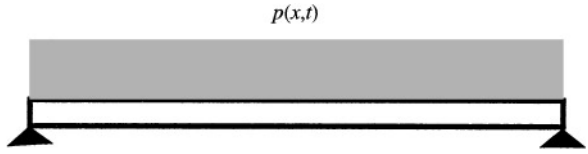

Figure 1. A simply supported beam under distributed loading $p(x, t)$.

of excitation pressure and local transverse velocity as

$$\pi_{\text{in}}(x) = \mathscr{R}e\left[\lim_{T\to\infty} \mathrm{E}\left\{\frac{1}{T} P(x,\omega,T)\,V^*(x,\omega,T)\right\}\right], \tag{1}$$

where P and V are the finite Fourier transforms of pressure $p(x,t)$ and transverse velocity $v(x,t)$ at position x, respectively, $\mathrm{E}\{\}$ denotes the expected value and * represents the complex conjugate operator. The complex transverse displacement of the structure obtained from modal analysis can be obtained by using

$$u(x) = \frac{1}{\rho A}\sum_{r=1}^{\infty} \frac{\phi_r(x)}{\omega_r^2 - \omega^2(1-\mathrm{j}\eta)} \int_0^L P(x')\phi_r(x')\,\mathrm{d}x', \tag{2}$$

where ρA is the mass per unit length of the beam, $\phi_r(x)$ is the shape of the rth mode, ω_r is the natural frequency of the rth mode, η is the internal loss factor, and $\mathrm{j} = \sqrt{-1}$. The dependence of spectral quantities, such as P and u, on the averaging time T and the frequency ω is not explicitly written in the following equations. The complex velocity $V(x)$ is

$$V(x) = \frac{\mathrm{j}\omega}{\rho A}\sum_{r=1}^{\infty} \frac{\phi_r(x)}{\omega_r^2 - \omega^2(1-\mathrm{j}\eta)} \int_0^L P(x')\phi_r(x')\,\mathrm{d}x'. \tag{3}$$

Substituting equation (3) for $V(x)$ into equation (1) yields

$$\pi_{\text{in}}(x) = \mathscr{R}e\left[\lim_{T\to\infty} \mathrm{E}\left\{\frac{1}{T} P(x)\frac{-\mathrm{j}\omega}{\rho A}\sum_{r=1}^{\infty} \frac{\phi_r(x)}{\omega_r^2 - \omega^2(1+\mathrm{j}\eta)} \int_0^L P^*(x')\phi_r(x')\,\mathrm{d}x'\right\}\right]. \tag{4}$$

Since $P(x')$ is the Fourier transform of the random pressure field at x', i.e.

$$P(x',\omega) = \int_{-T/2}^{T/2} p(x',t)\mathrm{e}^{-\mathrm{j}\omega t}\,\mathrm{d}t, \tag{5}$$

the input power density is

$$\pi_{\text{in}}(x) = \mathscr{R}e\left[\lim_{T\to\infty} \mathrm{E}\left\{\frac{1}{T}\int_{-T/2}^{T/2} p(x,t)\mathrm{e}^{-\mathrm{j}\omega t}\,\mathrm{d}t \times\frac{-\mathrm{j}\omega}{\rho A}\sum_{r=1}^{\infty} \frac{\phi_r(x)}{\omega_r^2 - \omega^2(1+\mathrm{j}\eta)} \int_0^L \int_{-T/2}^{T/2} p(x',t')\mathrm{e}^{\mathrm{j}\omega t'}\,\mathrm{d}t'\,\phi_r(x')\,\mathrm{d}x'\right\}\right]. \tag{6}$$

Exchanging the integration sequence of x' and t', making the change of variable $t' = t + \tau$, and using the definitions for the cross-correlation function

$$R(x,x',\tau) = \lim_{T\to\infty} \mathrm{E}\left\{\frac{1}{T}\int_{-T/2}^{T/2} p(x,t)p(x',t+\tau)\,\mathrm{d}t\right\} \tag{7}$$

and the cross-power spectral density

$$S_{xx'}(\omega) = \int_{-\infty}^{\infty} R(x,x',\tau)\mathrm{e}^{-\mathrm{j}\omega\tau}\,\mathrm{d}\tau, \tag{8}$$

allows the input power density to be written as

$$\pi_{\text{in}}(x) = \mathscr{R}e\left[\int_0^L S_{xx'}(\omega)\frac{-\mathrm{j}\omega}{\rho A}\sum_{r=1}^{\infty} \frac{\phi_r(x)\phi_r(x')}{\omega_r^2 - \omega^2(1+\mathrm{j}\eta)}\,\mathrm{d}x'\right], \tag{9}$$

where $S_{xx'}(\omega)$ is the cross-power spectral density between the pressures at positions x and x'. The transfer function between the excitation pressure at position x' and the velocity response at position x is

$$H_{xx'}(\omega) = \frac{\mathrm{j}\omega}{\rho A} \sum_{r=1}^{\infty} \frac{\phi_r(x)\phi_r(x')}{\omega_r^2 - \omega^2(1 - \mathrm{j}\eta)}. \tag{10}$$

The input power density for the beam at position x can therefore be written in terms of the transfer function $H_{xx'}$ as

$$\pi_{\mathrm{in}}(x) = \mathscr{R}e\left[\int_0^L S_{xx'}(\omega) H_{xx'}^*(\omega)\,\mathrm{d}x'\right]. \tag{11}$$

Similarly, for distributed loading on plates, the input power density at position $\mathbf{x} = (x, y)$ is

$$\pi_{\mathrm{in}}(\mathbf{x}) = \mathscr{R}e\left[\iint_S S_{\mathbf{xx}'}(\omega) H_{\mathbf{xx}'}^*(\omega)\,\mathrm{d}\mathbf{x}'\right], \tag{12}$$

where $S_{\mathbf{xx}'}$ is the cross-power spectral density between pressures at positions $\mathbf{x}$ and $\mathbf{x}'$. The transfer function can be expressed in terms of the natural modes of the plate as

$$H_{\mathbf{xx}'} = \frac{\mathrm{j}\omega}{\rho h} \sum_{m,n=1}^{\infty} \frac{\phi_{mn}(\mathbf{x})\phi_{mn}(\mathbf{x}')}{\omega_{mn}^2 - \omega^2(1 - \mathrm{j}\eta)}, \tag{13}$$

where ρh is the mass of the plate per unit area.

2.2. The Impedance Method

As an alternative approach to calculate the input power density, the impedance of the actual structure is approximated by that of a comparable structure of infinite extent. For multiple discrete random excitations, the power input to beams at the excitation point m can be expressed as (Han *et al.* 1997)

$$\pi_{\mathrm{in},m} = \frac{\omega}{4EIk^3} \sum_{n=1}^{N} \mathscr{R}e[S_{mn}(\omega)\alpha_{mn}], \quad m, n = 1, 2, \ldots, N, \tag{14}$$

where EI is the flexural rigidity, k is the wave number and N is the total number of input forces. The correction factor, α_{mn}, takes account of the interaction effect between the excitation forces at position m and n, due to waves propagating between these positions. For beams, the correction factor is given by

$$\alpha_{mn} = \left(1 + \mathrm{j}\,\frac{\eta}{4}\right)[\mathrm{e}^{\mathrm{j}k(1 + \mathrm{j}(\eta/4))|x_m - x_n|} + \mathrm{j}\mathrm{e}^{-k(1 + \mathrm{j}(\eta/4))|x_m - x_n|}]. \tag{15}$$

The power density input to the beam under distributed loading can thus be approximated as

$$\pi_{\mathrm{in}}(x) = \frac{\omega}{4EIk^3}\,\mathscr{R}e\left[\int_0^L S_{xx'}(\omega)\alpha_{xx'}\,\mathrm{d}x'\right], \tag{16}$$

where the correction factor, $\alpha_{\mathbf{x}\mathbf{x}'}$, is

$$\alpha_{xx'} = \left(1 + \mathrm{j}\,\frac{\eta}{4}\right)[\mathrm{e}^{\mathrm{j}k(1+\mathrm{j}(\eta/4))|x-x'|} + \mathrm{j}\mathrm{e}^{-k(1+\mathrm{j}(\eta/4))|x-x'|}]. \tag{17}$$

Similarly, the power density input to a plate can also be obtained using the impedance of an infinite plate. The power density input at position $\mathbf{x} = (x, y)$ can be expressed as

$$\pi_{\mathrm{in}}(\mathbf{x}) = \frac{1}{8(D\rho h)^{1/2}}\,\mathscr{R}e\left[\iint_S S_{\mathbf{x}\mathbf{x}'}(\omega)\alpha_{\mathbf{x}\mathbf{x}'}\,\mathrm{d}\mathbf{x}'\right], \tag{18}$$

where D is the bending stiffness of the plate. $8(D\rho h)^{1/2}$ is the impedance of the infinite plate. Assuming cylindrical travelling wave propagation in the plate, the correction factor, $\alpha_{\mathbf{x}\mathbf{x}'}$, is

$$\alpha_{\mathbf{x}\mathbf{x}'} = \left(1 + \mathrm{j}\,\frac{\eta}{2}\right)\left[\mathrm{H}_0^{(1)}\left(k\left(1 + \mathrm{j}\,\frac{\eta}{4}\right)r\right) - \mathrm{H}_0^{(1)}\left(\mathrm{j}k\left(1 + \mathrm{j}\,\frac{\eta}{4}\right)r\right)\right], \tag{19}$$

where $\mathrm{H}_0^{(1)}$ is the Hankel function of first kind and r is the distance between the position $\mathbf{x}$ and $\mathbf{x}'$.

The only approximation involved in the impedance method is that the impedance of an infinite structure is used. The impedance of a finite beam or plate varies from the impedance of an infinite beam or plate, especially at low frequency. Thus, the use of the impedance method may cause errors particularly at low frequency. The effects of this assumption will be investigated in Section 4.

Finally, the ordinary coherence, γ, between the fluctuating pressures at two different positions may be introduced into equations (16) or (18) through the relationship (Bendat & Piersol 1986)

$$\gamma^2 = \frac{|S_{\mathbf{x}\mathbf{x}'}|^2}{S_{\mathbf{x}\mathbf{x}}S_{\mathbf{x}'\mathbf{x}'}}. \tag{20}$$

3. DERIVATION OF THE ENERGY DENSITY RESPONSES

3.1. Energy Density Response from Modal Analysis

3.1.1. The response of beams

The response of beams and plates may be accurately obtained using the modal analysis method. The equation of motion for a damped flexible beam is

$$EI(1 + \mathrm{j}\eta)\frac{\partial^4 u}{\partial x^4} + \rho A\,\frac{\partial^2 u}{\partial t^2} = p(x, t), \tag{21}$$

where u is the normal beam displacement, η is the internal loss factor and $p(x, t)$ is the excitation pressure on the beam. Using the modal superposition approximation, the solution can be written as

$$u(x) = \sum_{r=1}^{\infty} u_r\phi_r(x), \tag{22}$$

where u_r is the coefficient for the rth mode, and ϕ_r is the corresponding eigenfunction. Substituting equation (22) into equation (21) yields the modal solution

$$(1 - \mathrm{j}\eta)\ddot{u}_r + \omega_r^2 u_r = \frac{q_r}{\rho A}, \tag{23}$$

where ω_r is the natural frequency of the rth mode. The modal force, q_r, is given by

$$q_r(t) = \int_0^L p(x,t)\phi_r(x)\,\mathrm{d}x. \tag{24}$$

Taking the Fourier transform of equation (23), solving for u_r, and substituting it into equation (22) gives the Fourier transform of the displacement

$$u(x,\omega) = \frac{1}{\rho A}\sum_{r=1}^{\infty}\frac{\phi_r(x)Q_r(x,\omega)}{\omega_r^2 - \omega^2(1 - \mathrm{j}\eta)}, \tag{25}$$

where Q_r is the Fourier transform of q_r. The power spectrum of the displacement can be written as

$$S_{uu} = \left(\frac{1}{\rho A}\right)^2 \sum_{r=1}^{\infty}\phi_r^2(x)|H_r(\omega)|^2 S_r(\omega), \tag{26}$$

where $H_r(\omega) = [\omega_r^2 - \omega^2(1 - \mathrm{j}\eta)]^{-1}$, $S_r(\omega)$ is the power spectrum of the generalized force for the rth mode, and all cross-modal terms have been neglected.

The power spectrum of the generalized force corresponding to the rth mode can be derived from the Fourier transform of the rth modal generalized force, equation (24), as

$$Q_r(x,\omega) = \int_{-T/2}^{T/2}\int_0^L p(x,t)\phi_r(x)\,\mathrm{d}x\,\mathrm{e}^{-\mathrm{j}\omega t}\,\mathrm{d}t. \tag{27}$$

The power spectrum of the rth modal force is

$$S_r(\omega) = \mathscr{R}e\left[\lim_{T\to\infty}\mathrm{E}\left\{\frac{1}{T}\int_0^L \phi_r(x_1)\int_{-T/2}^{T/2} p(x_1,t_1)\mathrm{e}^{-\mathrm{j}\omega t_1}\,\mathrm{d}t_1\,\mathrm{d}x_1 \times \int_0^L \phi_r(x_2)\int_{-T/2}^{T/2} p(x_2,t_2)\mathrm{e}^{\mathrm{j}\omega t_2}\,\mathrm{d}t_2\,\mathrm{d}x_2\right\}\right]. \tag{28}$$

Interchanging the order of integration, making the change of variable $t_1 = t_2 + \tau$, and using the definitions of the cross-correlation function [equation (7)] and the cross-power spectral density [equation (8)] yields the power spectrum of the generalized force:

$$S_r(\omega) = \mathscr{R}e\left[\int_0^L\int_0^L \phi_r(x_1)\phi_r(x_2)S_{x_1x_2}(\omega)\,\mathrm{d}x_1\,\mathrm{d}x_2\right], \tag{29}$$

where $S_{x_1x_2}$ is the cross-spectral density between the pressure at positions x_1 and x_2. The power spectrum of the normal displacement of the beam is then found by substituting equation (29) into equation (26),

$$S_{uu} = \frac{1}{(\rho A)^2}\sum_{r=1}^{\infty}|H_r(\omega)|^2\phi_r^2(x) \times \mathscr{R}e\left[\int_0^L\int_0^L \phi_r(x_1)\phi_r(x_2)S_{x_1x_2}(\omega)\,\mathrm{d}x_1\,\mathrm{d}x_2\right]. \tag{30}$$

The mean square value of the displacement can be obtained by integrating the power spectrum over the frequency range

$$\overline{u^2(x)} = \frac{1}{\pi}\frac{1}{(\rho A)^2}\sum_{r=1}^{\infty}\phi_r^2(x)\times\int_0^{\infty}|H_r(\omega)|^2\,\mathscr{R}e\left[\int_0^L\int_0^L\phi_r(x_1)\phi_r(x_2)S_{x_1x_2}(\omega)\,\mathrm{d}x_1\,\mathrm{d}x_2\right]\mathrm{d}\omega, \quad (31)$$

where the overbar denotes time averaging. Assuming pure bending waves, the total energy response of the beam is the sum of the kinetic energy and the potential energy

$$e = \frac{1}{2}\rho A\overline{v^2(x)} + \frac{1}{2}\mathrm{EI}\overline{(\partial^2 u/\partial x^2)^2}, \quad (32)$$

where $v(x)$ is the velocity distribution. Both $v(x)$ and $\partial^2 u/\partial x^2$ can be derived from $u(x)$.

3.1.2. The response of plates

The exact energy density response of a plate under distributed loading can be obtained following a similar procedure. The mean square value of the transverse displacement is

$$\overline{u^2(\mathbf{x})} = \frac{1}{\pi}\frac{1}{(\rho h)^2}\sum_{m,n=1}^{\infty}\phi_{mn}^2(\mathbf{x})\int_0^{\infty}|H_{mn}(\omega)|^2 \times\iint_{S_2}\iint_{S_1}\phi_{mn}(\mathbf{x}_2)\phi_{mn}(\mathbf{x}_1)\mathscr{R}e[S_{\mathbf{x}_1\mathbf{x}_2}(\omega)]\,\mathrm{d}\mathbf{x}_1\,\mathrm{d}\mathbf{x}_2\,\mathrm{d}\omega, \quad (33)$$

where $H_{mn}(\omega) = [\omega_{mn}^2 - \omega^2(1 - \mathrm{j}\eta)]^{-1}$. The kinetic energy of a plate is

$$T = \tfrac{1}{2}\rho h\overline{v^2(x)}. \quad (34)$$

The kinetic energy can be calculated readily from the displacement solution. Furthermore, in the far field the kinetic energy and potential energy are approximately equal, as discussed by Bouthier & Bernhard (1995*b*). Hence, the total energy may be approximated as

$$e = 2T = \rho h\overline{v^2(\mathbf{x})}. \quad (35)$$

3.2. Energy Flow Analysis

The equation governing the energy distribution of flexural waves in a transversely vibrating beam has the form (Wohlever & Bernhard 1992)

$$-\frac{c_g^2}{\eta\omega}\frac{\mathrm{d}^2 e}{\mathrm{d}x^2} + \eta\omega e = \pi_{\mathrm{in}}, \quad (36)$$

where e is the time-averaged and smoothed energy density, c_g is the group velocity of flexural waves and π_{in} is the input power density. For thin, transversely vibrating plates where the wave field can be assumed to be superposition of plane waves, the governing equation is (Bouthier & Bernhard 1995b)

$$-\frac{c_g^2}{\eta\omega}\left(\frac{\partial^2}{\partial x^2} + \frac{\partial^2}{\partial y^2}\right)e + \eta\omega e = \pi_{\mathrm{in}}. \quad (37)$$

For all of the case studies shown in this paper, the intensity input is wide band. Hence, the total energy density is calculated by integrating the energy density over the frequency range

$$e_{\text{total}} = \int_{\omega_1}^{\omega_2} e \, \mathrm{d}\omega. \tag{38}$$

For numerical implementation, this integral is written as

$$e_{\text{total}} = \sum_{\omega_1}^{\omega_2} e \delta\omega, \tag{39}$$

where e can be obtained by solving the energy flow analysis equations [equations (36) and (37)].

The EFA model for beams is shown in Figure 2. The beam is simply supported at its ends. Thus, the flux of energy at the ends is zero since both the displacement and the bending moment are zero there. For a beam of length L, the energy density e can be assumed to be

$$e = \sum_{r=0}^{\infty} A_r \cos \frac{r\pi x}{L}. \tag{40}$$

The basis function $\cos(r\pi x/L)$ satisfies the energy boundary conditions. The input power densities can be calculated from the transfer function method or the impedance method developed in Section 2. Using Fourier analysis, the input power density can be expanded in terms of the basis function as

$$\pi_{\text{in}} = \sum_{r=0}^{\infty} B_r \cos \frac{r\pi x}{L}, \tag{41}$$

where

$$B_r = \int_0^L \pi_{\text{in}}(x) \cos \frac{r\pi x}{L} \, \mathrm{d}x. \tag{42}$$

Using equation (36), the energy density is

$$e = \sum_{r=0}^{\infty} \frac{B_r \cos(r\pi x/L)}{(c_g^2/\eta\omega)(r\pi/L)^2 + \eta\omega}. \tag{43}$$

For the corresponding plate vibration problems, the energy density calculated by EFA is

$$e = \sum_{m,n=0}^{\infty} \frac{B_{mn} \cos(m\pi x/L_x)\cos(n\pi y/L_y)}{(c_g^2/\eta\omega)[(m\pi/L_x)^2 + (m\pi/L_y)^2] + \eta\omega}, \tag{44}$$

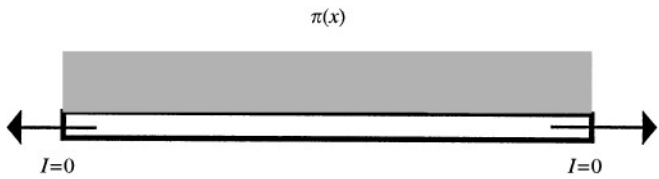

Figure 2. EFA model of a beam under distributed power density input.

where

$$B_{mn} = \int_0^{L_y} \int_0^{L_x} \pi_{\text{in}}(x, y) \cos \frac{m\pi x}{L_x} \cos \frac{n\pi y}{L_y} \, \mathrm{d}x \, \mathrm{d}y, \tag{45}$$

and L_x and L_y are the dimensions of the plate.

4. RESULTS

The energy density response of simply supported beams and plates was obtained using modal analysis and EFA, with both the transfer function and impedance methods for calculating the power density input.

4.1. Beam Response

The case of the uniform beam simply supported at both ends, excited by a distributed pressure field was first considered (Figures 1 and 2). The auto-spectral density of the fluctuating pressure was assumed to have a Gaussian distribution over frequency, with a centre frequency of 500 Hz and a half-power bandwidth of 230 Hz. This was to avoid excitation of lower-order modes which overwhelmed the higher-order modal response of interest. The mean square value of the pressure was $5{\cdot}0 \times 10^{-5}$ N^2/m^4. The beam parameters were $E = 7{\cdot}1 \times 10^{10}$ N/m^2, $A = 0{\cdot}0001$ m^2, $\rho = 2700$ Kg/m^3, $I = 8{\cdot}33 \times 10^{-10}$ m^4, $\eta = 0{\cdot}2$, and $L = 1{\cdot}0$ m.

For the numerical implementation of the modal analysis method, a total of 70 modes were used to ensure satisfactory convergence of the solution. Results were obtained with and without including the cross-modal terms. For the EFA method, the input power densities were calculated using both the transfer function method and the impedance method. The energy density was calculated over the frequency range 0–1000 Hz. The frequency range was divided into 200 frequency bands, with a resolution bandwidth of 5 Hz. The energy density for each frequency component was calculated from equation (43). The total energy density response was obtained by summing the energy density for each frequency component using equation (39).

The cross-power spectral density of the wall pressure fluctuations was assumed to have the form of the Corcos model (Blake 1986), commonly used for flow-excited structural vibration problems. The coherence in the streamwise and spanwise directions is assumed to decay exponentially with distance (Corcos 1967), i.e.

$$\gamma = \mathrm{e}^{-\alpha |\omega(x - x')/U_c|}, \tag{46}$$

where U_c is the turbulence convection speed, and α is the decay constant. In this case study, $U_c = 35$ m/s and $\alpha = 0{\cdot}18$.

Figure 3 shows the input power density distribution calculated using both the transfer function method and the impedance method. The power density distribution obtained using the transfer function method, which is accurate since it includes the effects of boundaries, oscillates with position. The approximate result (neglecting the effects of boundaries) obtained from the impedance method is nearly uniform. Overall, however, the two methods are in good general agreement. The approximate method slightly underestimates (by about 1 dB) the input power density near the centre of the beam. As expected, larger discrepancies occur within a few wavelengths from the boundaries.

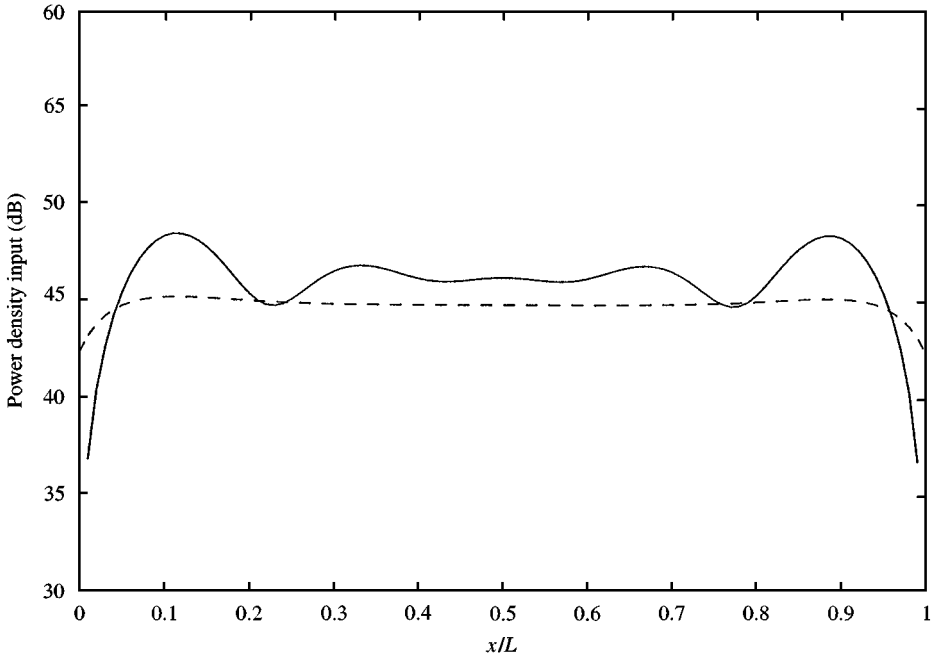

Figure 3. The power density input distribution over the beam: ——, the transfer function method; – – – –, the impedance method. The reference power density is 1×10^{-12} W/m.

Figure 4 shows the energy density response of the beam. Two of the results shown were obtained using modal analysis: one including the cross-modal terms and one neglecting the cross-modal terms. The other two results are for EFA: one using the transfer function method, and the other using the impedance method for calculating input power density. There are differences between the two results for the modal analysis method. The errors involved, however, are not very significant. This indicates that the cross-modal terms in the exact solution may be neglected in this case. In the central region of the beam, the modal analysis solutions and the approximate EFA solutions are in very good agreement, i.e. within 1 dB. There are differences between the modal analysis solutions and the approximate EFA solutions near the boundaries, where the exact solution tends towards zero (in agreement with the boundary conditions) while the approximate solutions are nearly constant. However, the EFA solution is a good representation of the spatially averaged response. The difference between the two EFA results is less than 1 dB. The impedance method is thus a good approximation of the power density input.

4.2. The Plate Response

The plate was assumed to be simply supported along its edges and excited by a distributed pressure field over the whole plate. The auto-spectral density of the pressure was assumed to be uniform, and consisted of band-limited white noise within the one-third octave band centred at 500 Hz. This spectral distribution was chosen in order to avoid the excitation of lower-order modes, which tended to overwhelm the high-frequency structural response of interest. The mean square value of the pressure at each position was 5×10^{-3} N^2/m^4. The

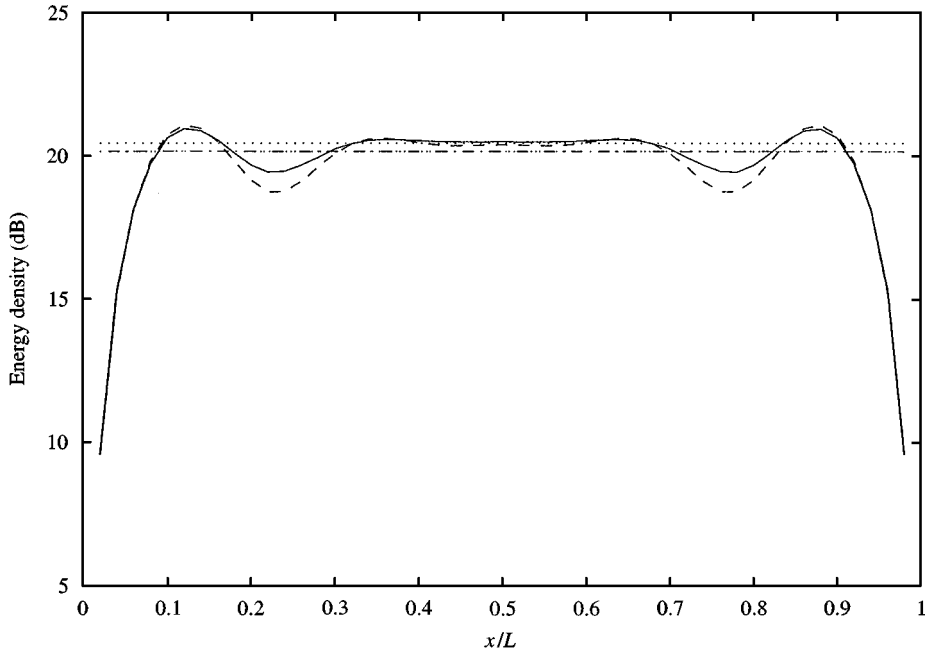

Figure 4. The energy density distribution over the beam: ——, modal analysis method, considering cross terms; – – – –, modal analysis method, neglecting cross terms; –·–·–, EFA/transfer function method; ...., EFA/impedance method. The reference energy density is 1×10^{-12} J/m.

parameters of the plate were $E = 7{\cdot}1 \times 10^{10}$ N/m^2, $\rho = 2700$ kg/m^3, $h = 0{\cdot}001$ m, $L_x = L_y = 1{\cdot}0$ m, $\eta = 0{\cdot}2$, and $\sigma = 0{\cdot}3$.

The input power density over the excitation region was calculated using both the transfer function method and the impedance method. The energy density was obtained using both modal analysis and the approximate EFA method. For the modal analysis method, a total of 400 modes were used, which ensured convergence for this case. For EFA, the energy density was computed over the one-third octave band centred at 500 Hz. The frequency range was divided into 10 subbands with a bandwidth of approximately 11 Hz each.

Following the Corcos model, the coherence of the excitation pressure was assumed to be

$$\gamma = \mathrm{e}^{-\alpha|\omega(x-x')/U_c|}\mathrm{e}^{-\beta|\omega(y-y')/U_c|}, \tag{47}$$

where the decay rate coefficients α and β were obtained from experimental results (Han 1997), $\alpha = 0{\cdot}18$, $\beta = 0{\cdot}80$ and the convection speed was $U_c = 35$ m/s.

Figure 5 shows the input power density distribution over the plate calculated using the transfer function method. The input power density results calculated using the impedance method are shown in Figure 6. As for the beam, the more accurate transfer function solution exhibits oscillations near the boundaries. It is uniform in the central region of the plate. Note that the input power density reaches zero at the edges, which is not shown in Figure 5. The approximate input power density calculated using the impedance method is almost uniform over the plate. The results obtained from the two methods are in good general agreement, especially in the centre. This indicates that the approximate method of calculating input power density approximating the impedance by that of a comparable structure of

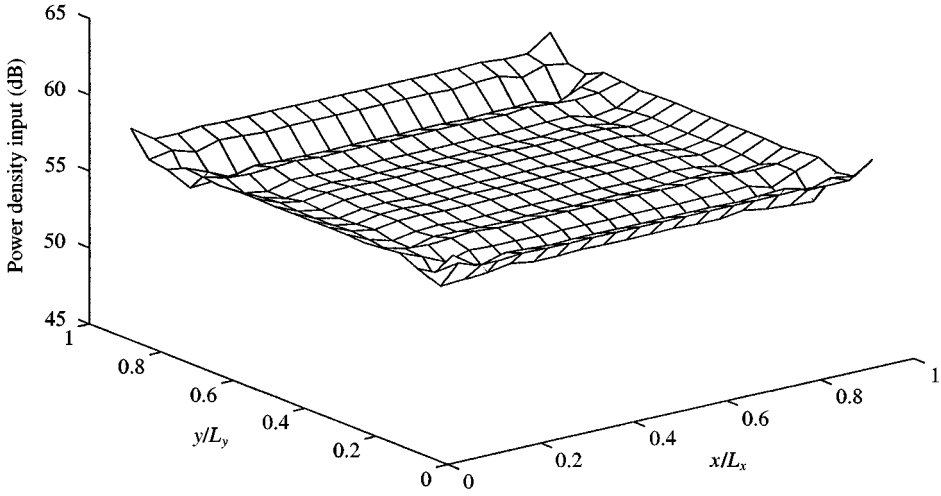

Figure 5. The power density input distribution over the plate using the transfer function method. The reference power density is 1×10^{-12} W/m^2.

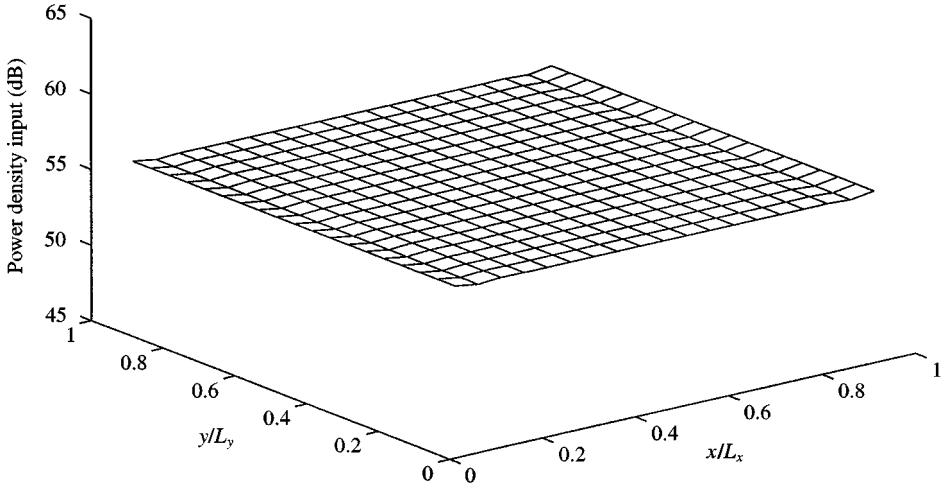

Figure 6. The power density input distribution over the plate using the impedance method. The reference power density is 1×10^{-12} W/m^2.

infinite extent is accurate at high frequency, within 1 or 2 dB. Power density input calculations using the transfer function method requires knowledge of the modal response of the structure, whereas the impedance method requires only local information. The computational effort for calculating the power density input to a system is greatly reduced using the impedance method.

The energy density distribution computed from EFA and the transfer function method is shown in Figure 7. The results using EFA and the impedance method are shown in Figure 8. The two approximate energy density results are similar, and both are almost uniformly distributed over the plate.

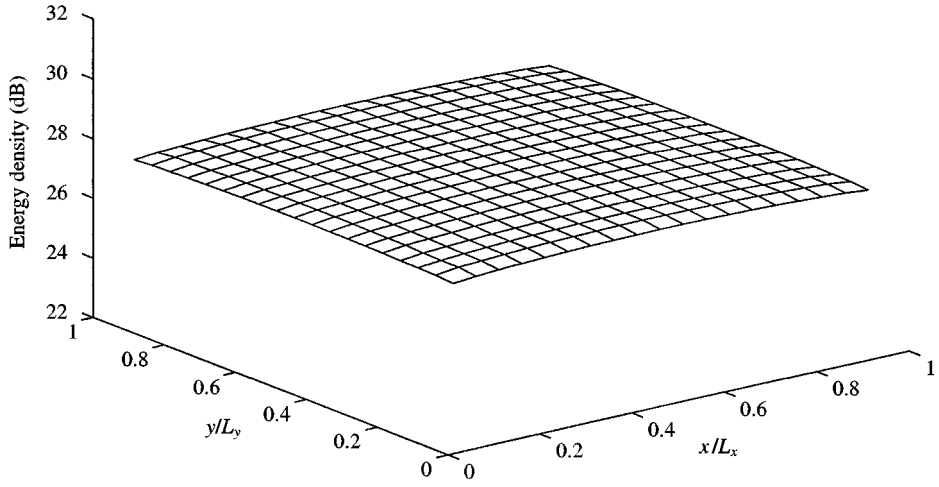

Figure 7. The energy density distribution over the plate using EFA and the transfer function method. The reference energy density is 1×10^{-12} J/m^2.

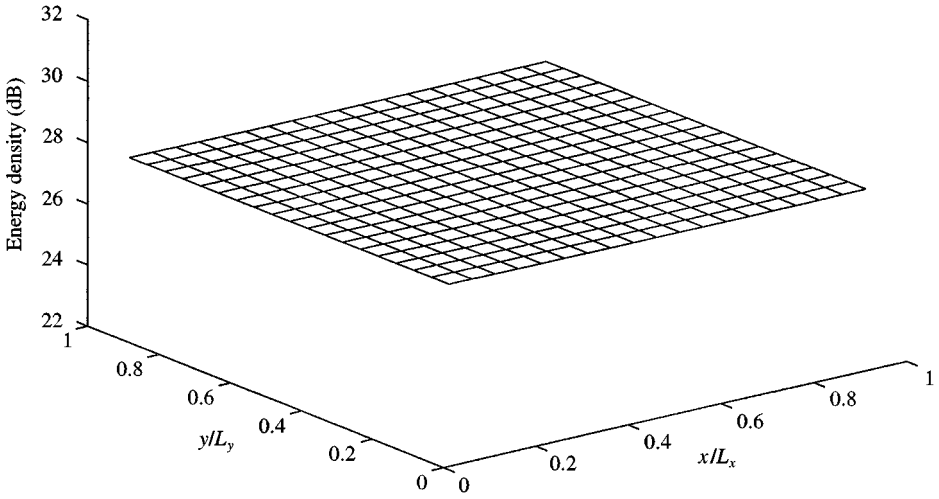

Figure 8. The energy density distribution over the plate using EFA and the impedance method. The reference energy density is 1×10^{-12} J/m^2.

The energy density distribution calculated using modal analysis is shown in Figure 9. The energy density is relatively uniform in the centre of the plate. The energy density increases close to the boundaries. This is probably an artefact of the assumption that the potential energy and the kinetic energy are equal. This assumption breaks down near the plate boundary.

In order to illustrate the difference between the exact solutions and the EFA approximations, the energy responses along the diagonal line $x = y$ are shown in Figure 10. The difference between the two EFA predictions is slight. The energy density prediction

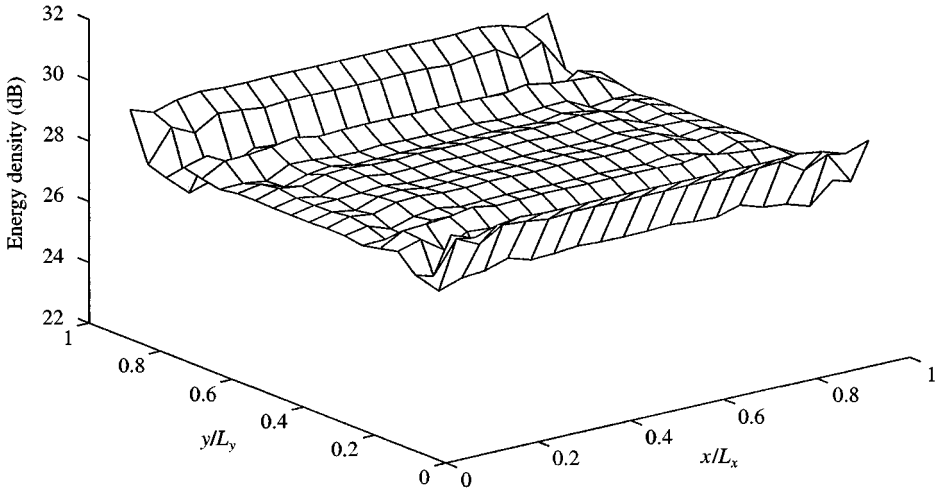

Figure 9. The energy density distribution over the plate using modal analysis method. The reference energy density is 1×10^{-12} J/m^2.

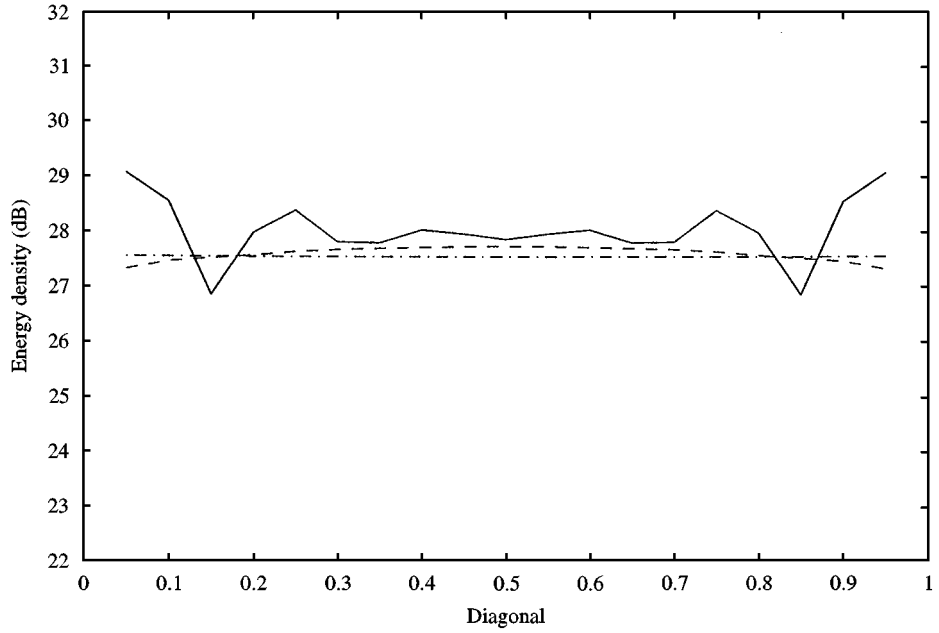

Figure 10. The energy density distribution along the diagonal: —— modal analysis method; – – – –, EFA/transfer function method; – . – . – . –, EFA/impedance method. The reference energy density is 1×10^{-12} J/m^2.

obtained using the impedance method is almost uniform, whereas that obtained using the transfer function method tends to decrease close to the boundaries because the exact power density input is zero at the edges. In the central region of the plate, the modal analysis solution and the EFA solutions are in good agreement. The exact solution oscillates near

the boundaries, whereas the EFA results are almost uniform. This phenomenon is typical of the results reported in previous studies for simple harmonic and local excitation forces (Bouthier & Bernhard 1995*a*, *b*) and occurs because the EFA does not model the near-field of boundaries. However, the EFA results are good representations of the spatially averaged response.

5. APPLICATION OF THE METHOD TO UNEVENLY DISTRIBUTED EXCITATIONS

The approximate energy method was used to predict the energy response of a simply supported square plate excited by a turbulent boundary layer over half of the span of the plate, as shown in Figure 11. The power density input to the plate was calculated from the measured cross-power spectral density of the wall pressure. The surface pressure auto-power spectral density for air flow over a flat, rigid plate was measured in a low-speed, quiet wind tunnel using an array of microphones for various flow speeds (Han 1997). The power spectra at different flow speeds were cast in nondimensional form, and collapsed into a single curve for the entire frequency range of interest when scaled by outer boundary-layer flow variables. The results are shown in Figure 12. An empirical model of the wall pressure power spectra can be obtained by fitting the curve. The model is

$$\Phi(\omega) = \begin{cases} 1\times 10^{-5}\,\rho^2\delta^* U_0^3 \left(\dfrac{\omega\delta^*}{U_0}\right)^{-0\cdot5}, & \dfrac{\omega\delta^*}{U_0} < 1\cdot5, \\ 1\times 10^{-4}\,\rho^2\delta^* U_0^3 \left(\dfrac{\omega\delta^*}{U_0}\right)^{-5}, & \dfrac{\omega\delta^*}{U_0} > 1\cdot5, \end{cases} \tag{48}$$

where $\Phi(\omega)$ is the auto-power spectral density of pressure, U_0 is the free-stream velocity, ρ is the air density and δ^* is the displacement thickness of the boundary layer. A comparison of this empirical model and the experimental results is shown in Figure 12. At low frequencies, the spectra exhibit a $\omega^{-0\cdot5}$ trend, while at high frequency the trend is ω^{-5}. This is slightly different from the modal suggested by Skudrzyk & Haddle (1960), in which the power spectrum is a constant in low frequency.

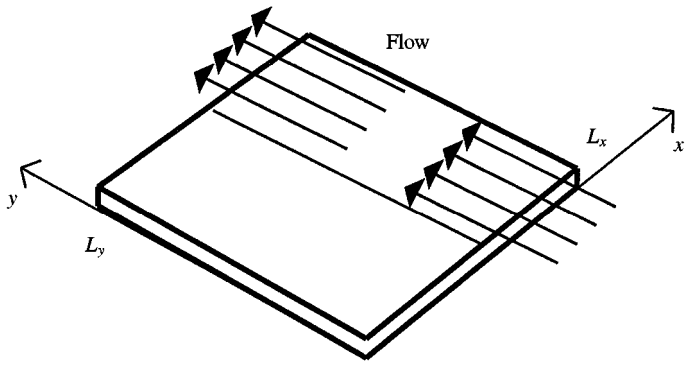

Figure 11. A simply supported plate excited by turbulent flow in the half region.

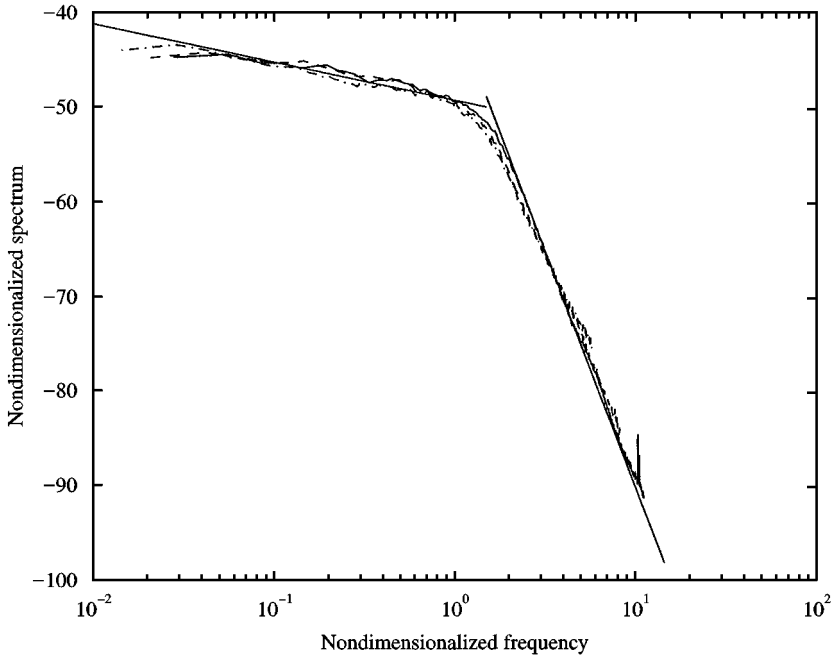

Figure 12. Auto-power spectral densities of wall pressure scaled by outer layer variables for various flow speeds. $\Phi(\omega)/(\rho\delta^{*}U_0^3) \sim \omega\delta^{*}U_0$. ——, $U_0 = 15$ m/s; – – – –, $U_0 = 25$ m/s; –.–.–.–, $U_0 = 30$ m/s. The straight line is the empirical model.

Using the Corcos model, the coherence in the streamwise direction was assumed to be

$$\gamma(\xi, \omega) = \mathrm{e}^{-\alpha|\omega\xi/U_c|}, \tag{49}$$

and in the spanwise direction, it was

$$\gamma(\eta, \omega) = \mathrm{e}^{-\beta|\omega\eta/U_c|}, \tag{50}$$

where ξ and η are streamwise and spanwise distances, respectively, U_c is the convection speed and α and β are two constants depending on the smoothness of the wall. The streamwise coherence spectra for different spacings when flow free-stream velocity is 25 m/s are plotted in Figure 13, as a function of $\omega\xi/U_c$;U_c was assumed to be a constant, $U_c = 0{\cdot}65U_0$. The scaled coherence spectra collapse approximately to a single curve at high frequency. The decay rate, α, was obtained by fitting the curve using the Corcos model. A decay rate of 0·18 was obtained. Note that the Corcos model does not yield a very accurate prediction of coherence in this case (a polynomial expression would be better). This may be due to the fact that the outer flow was a duct flow (i.e. an effect of wind-tunnel wall containment). Nevertheless, the Corcos model was selected for simplicity. It is believed that the associated inaccuracies did not have a strong impact on the accuracy of the predicted energy density. A similar approach was used to determine the decay rate along spanwise direction, β. In this case, $\beta = 0{\cdot}80$ was found. The cross-power spectral density of wall pressures is therefore

$$S_{\mathbf{x}\mathbf{x}'}(\omega) = \Phi(\omega)\mathrm{e}^{-0{\cdot}18|\omega(y-y')/U_c|}\mathrm{e}^{-0{\cdot}8|\omega(x-x')/U_c|}\mathrm{e}^{-\mathrm{j}(\omega(y'-y)/U_c}. \tag{51}$$

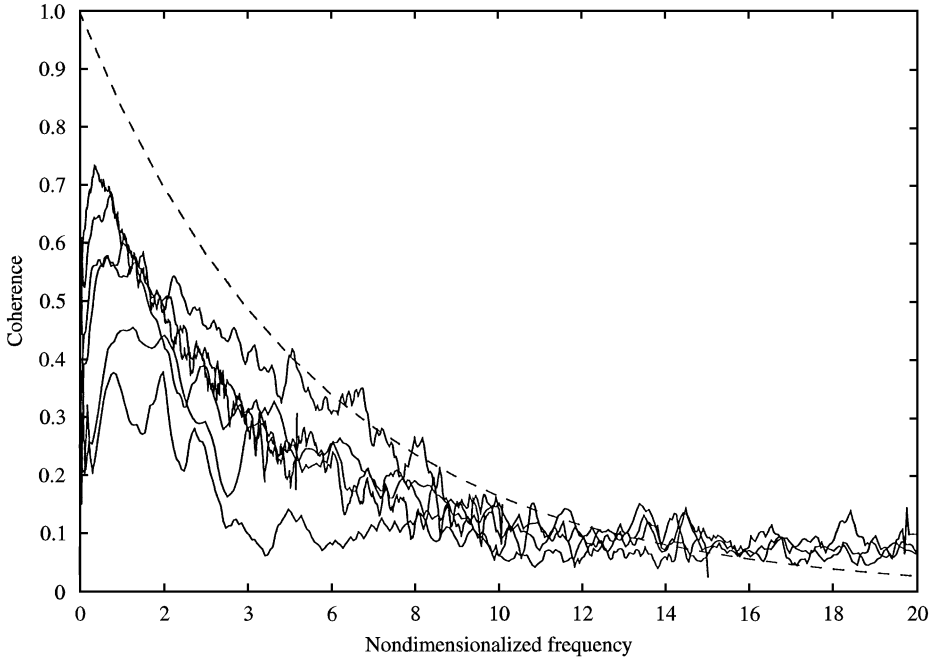

Figure 13. Streamwise coherence versus $\omega\xi/U_c$ with $U_0 = 25$ m/s for a range of spacings. – – – –, Corcos model with $\alpha = 0{\cdot}18$.

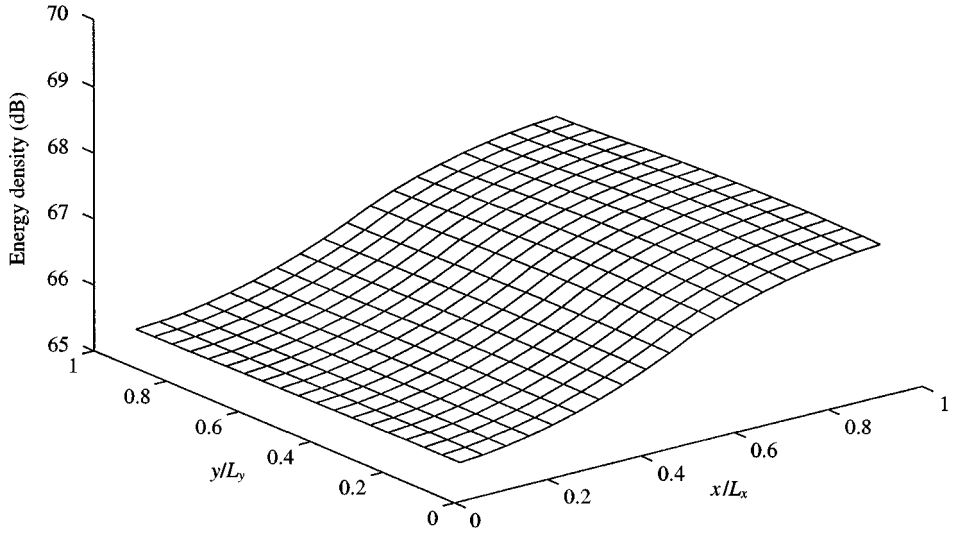

Figure 14. The approximate energy response of the plate excited by turbulent flow in half of the span of the plate. The reference energy density is 1×10^{-12} J/m^2.

The approximate energy response of the plate wetted over half of the plate in the spanwise direction was obtained for a free-stream velocity of 25 m/s. The results are shown in Figure 14. It can be seen that the energy density decays smoothly between the excitation region and the unexcited region, as expected. The EFA method captures this trend, and thus yields

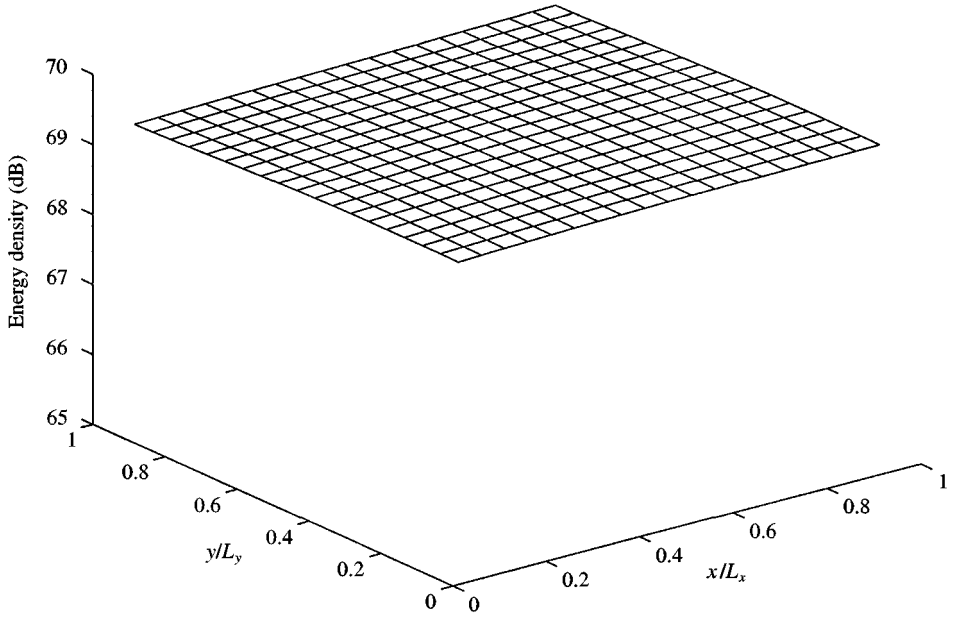

Figure 15. The approximate energy response of the plate fully covered with turbulent flow. The reference energy density is 1×10^{-12} J/m^2.

more detailed spatial information than SEA. The energy response when the plate is fully covered by turbulent boundary layer flow was also calculated and is shown in Figure 15. In this case, the response is much more uniform over the plate and is slightly higher about 2 dB than that in the excitation region for half-coverage.

6. CONCLUSIONS

Two methods for calculating the power density input to vibrating beams and plates excited by a distributed fluctuating pressure field have been developed: the transfer function method and the impedance method. The input power density was expressed in terms of the cross-power spectral density of the fluctuating pressures. The coherence condition, therefore, is included in the expressions for the input power density. The methods for calculating the input power density and the energy flow analysis method for calculating the energy density responses were compared to modal analysis results. The impedance method of calculating the input power density is a good approximation of the exact transfer function method. The energy flow analysis was also used to predict the energy response of a plate excited by a turbulent boundary-layer flow over half the plate span. The results showed that energy flow analysis can be used to predict the space averaged energy response of a structure excited by random distributed fluctuating pressure fields, such as wall pressure field under turbulent boundary layer.

ACKNOWLEDGEMENTS

The authors wish to express their appreciation to the Purdue Research Foundation for its financial support of this work. Some of the material in this paper was presented as an

ASME conference paper at the *Fluid and Structure Interaction, Aero-elasticity & Flow-Induced Vibration and Noise Symposium*, at the 1997 ASME International Engineering Congress and Exposition in Dallas, Texas, in November 1997.

References

Bendat, J. S. & Piersol, A. G. 1986 *Random Data Analysis and Measurement Procedures*. New York: Wiley.

Blake, W. K. 1986 *Mechanics of Flow-Induced Sound and Vibration*. Orlando: Academic Press.

Bouthier, O. M. & Bernhard, R. J. 1995*a* Simple models of the energy flow in vibrating membranes. *Journal of Sound and Vibration* **182,** 129–147.

Bouthier, O. M. & Bernhard, R. J. 1995*b* Simple models of the energetics of transversely vibrating plates. *Journal of Sound and Vibration* **182,** 149–164.

Corcos, G. M. 1967 The resolution of turbulent pressures at the wall of a boundary layer. *Journal of Sound and Vibration* **6,** 59–70.

Crandall, S. H. & Mark, W. D. 1963 *Random Vibration in Mechanical Systems*. London: Academic Press.

Cremer, L. & Heckl, M. 1988 *Structure-borne Sound*. New York: Springer.

Fahy, F. 1985 *Sound and Structural Vibration*: *Radiation, Transmission, and Response*. London: Academic Press.

Han, F. 1997 Measurement of pressure fluctuations under turbulent boundary layer. Ray W. Herrick Laboratories Internal Report-213, HL 97-14, Purdue University.

Han, F., Bernhard, R. J. & Mongeau, L. G. 1997 Energy flow analysis of vibrating beams and plates for discrete random excitations. *Journal of Sound and Vibration* **208,** 841–859.

Skudrzyk, E. J. & Haddle, G. P. 1960 Noise reduction in a turbulent boundary layer by smooth and rough surfaces. *Journal of the Acoustical Society of America* **32,** 19–34.

Wohlever, J. C. & Bernhard, R. J. 1992 Mechanical energy flow models of rod and beams. *Journal of Sound and Vibration* **153,** 1–19.